Nanochem. Res., 9(1): 42-54, Winter 2024

RESEARCH PAPER

Synthesis of nanochitosan from Cambarus bartonii waste and its utilization in the removal of polycyclic aromatic hydrocarbons in surface water from Ifite Ogwari, Southeastern Nigeria

Vincent Nwalieji Okafor[1,*], Deborah Oluwalana Kehinde[1], Abimbola Bankole Akinyele[1] and Benjamin Uchenna Modozie[2]

[1]Department of Pure and Industrial Chemistry, Nnamdi Azikiwe University, Awka, Nigeria
[2]Department of Pharmaceutical and Medicinal Chemistry, Nnamdi Azikiwe University, Awka, Nigeria

ARTICLE INFO

Article History:
Received 17 Aug 2023
Accepted 05 Dec 2023
Published 01 Jan 2024

Keywords:
Biowaste,
Crayfish,
Water treatment,
Nanoparticles,
Characterization.

ABSTRACT

Access to potable water is a global problem, especially in rural communities of the world. Ifite Ogwari is a rural community in Southeastern Nigeria that depends mostly on surface water for its water needs such as drinking. This work explored the use of nanochitosan for removing polycyclic aromatic hydrocarbons (PAHs) contained in the surface water obtained from Ifite Ogwari. Chitosan extracted from C*ambarus bartonii* waste (CbC) and artificial chitosan (ArC) supplied by ChitoLytic were reduced to nanochitosan particles. The nanochitosan particles were characterized using Dynamic Light Scattering (DLS), also known as Photon Correlation Spectroscopy, Fourier Transformed Infrared Spectroscopy (FTIR), Scanning Electron Microscopy (SEM), and X-ray Diffraction (XRD). PAHs were assessed in untreated and treated water samples using Gas Chromatography-Flame ionization Detector (GC-FID). Results of DLS particle size analyzer ranged between 55.78 nm and 92.64 nm. FTIR gave bands at 2922.2 cm^{-1} and 1405.2 cm^{-1} representing C–H and C–N groups, respectively, while the band at 1025.0 cm^{-1} stretches C–O–C groups. SEM results show interconnected microporosity while XRD results demonstrate sharp peaks at 2θ = 8.20°, 32.08°, 38.00° and 45.76° for nanochitosan from C*ambarus bartonii* waste (CbNC) and 2θ = 20.21°, 31.63° and 45.48° for nanochitosan from artificial chitosan (ArNC). Nine PAHs were detected in the untreated water while seven were below detectable limit but none was detected in the treated water samples. This study indicates that nannochitosan synthesized from *C. bartonii* waste could be used for the removal of PAHs from contaminated surface water.

How to cite this article
Okafor V. N., Kehinde D. O., Akinyele A. B., Modozie B. U., Synthesis of nanochitosan from Cambarus bartonii waste and its utilization in the removal of polycyclic aromatic hydrocarbons in surface water from Ifite Ogwari, Anambra State, Nigeria. Nanochem. Res., 2024; 9(1): 42-54. DOI: 10.22036/NCR.2024.01.06

INTRODUCTION

Water resources around the world could contain a variety of contaminants that, at high concentrations, could increase the risk of contracting a number of diseases in both adults and children, including serious diseases like gastrointestinal illnesses, developmental effects such as cognitive disorders, endocrine disruption, and cancer [1]. The primary sources of drinking water in the majority of rural communities in Nigeria include surface water, such as rivers, lakes, and reservoirs, as well as groundwater aquifers, which are subsurface layers of permeable soil and rock that contain substantial amounts of water. The rural community of Ifite Ogwari in Anambra State is not an exception.

Previous works by Okafor and co-workers indicated that surface and groundwater sources from Ifite Ogwari are polluted by heavy metals and

* Corresponding Author Email: *vnw.okafor@unizik.edu.ng*

polycyclic aromatic hydrocarbons [2, 3]. Scholars recently have also found PAHs as well as heavy metals in food and food products [4 - 6], beverages [7 – 10], meat and meat products [11, 12] etc.

Globally, there exist many polycyclic aromatic hydrocarbons, primarily because of persistent anthropogenic pollution sources. As a result of their innate characteristics, including hydrophobicity, thermostability, and heterocyclic aromatic ring structures, PAHs are resistant and extremely persistent in the environment. For a variety of living forms, PAH pollution have been found to be extremely toxic, mutagenic, carcinogenic, teratogenic, and immunotoxicogenic [13-15].

Chitosan, a linear polysaccharide composed of randomly distributed β-(1→4)-linked d-glucosamine and N-acetyl-d-glucosamine has been applied in the treatment of wastewater and water bodies contaminated with heavy metals [16, 17]. Chitosan is also employed in drug manufacturing and numerous other applications such as normalizing blood pressure and cholesterol levels, treating obesity, speeding up the healing of wounds, and as flocculant, coagulant, food additive, weight loss, etc. [18]. The literature abounds with numerous studies on the use of chitosan as a flocculant, coagulant, and as adsorbent for removing contaminants such as heavy metals, dyes, pesticides, antibiotics as well as biological contaminants from wastewater [19 – 21].

The aim of the present study is to adsorb the PAHs in surface water obtained from Ifite Ogwari using synthesized nanochitosan. Previous researches have covered the use of chitosan for wastewater treatment [19 – 21]. Nonetheless, there is little or no existing literature on the extraction of nanochitosan from *Cambarus bartonii* waste for the treatment of surface water from any Nigerian rural community.

EXPERIMENTAL SECTION

Procurement of raw materials

Crayfish waste obtained from Eke-Awka market was made free from dirt before it was pulverized into powder using a dry grinder and sieved with a 2mm sieve. Low molecular weight chitosan (artificial chitosan) was supplied by ChitoLytic from North America. Chemicals and reagents used were potassium hydroxide (KOH), acetic acid (CH_3COOH), hydrochloric acid (HCl), sodium hydroxide (NaOH), lead nitrate ($Pb(NO_3)_2$), sodium acetate (CH_3COONa), sodium tripolyphosphate ($Na_5P_3O_{10}$), dihydrogen phosphate (H_2PO_4), distilled water etc. All reagents used were of analytical grade.

Extraction of Chitin and Chitosan

Chitosan was prepared following the method described by Okoya *et al.* [22] with modifications as adapted by Okafor *et al.* [23]. The crayfish waste was pulverized into powder using a dry grinder and sieved with 2 mm sieve. 50 g of powdered crayfish waste, with a particle size of less than 2 mm, were weighed into a 500 mL beaker, and 200 mL of 4% (w/v) NaOH was added with constant stirring for 6 h at 80 °C and filtered. The residue was washed with distilled water until it was free of base and then dried at 100 °C for 2 h. The deproteinized crayfish waste residue was then poured into a 250 mL conical flask and 100 mL of 3 % (v/v) 1 mol/dm^3 HCl was added and placed on a magnetic stirrer for 3 h at 30°C to demineralize it. The content was filtered and the residue washed until it was free of acid. The acid free residue was then dried at 90 °C for 1 h. A snow-white residue called chitin was obtained. The chitin was poured into a 250 mL conical flask for deacetylation. A 50% (w/v) NaOH solution was added, stirred at 30°C for 4 h and filtered. After filtration, the residue, which is chitosan was washed until the filtrate was neutral and dried at 90°C for 1 h, then stored for further studies.

Chitosan Modification

A 1M H_2PO_4 was added to 100 g of chitosan and allowed to stand for 30 min and after which the liquid was discarded. The wet chitosan was spread on a stainless-steel tray and dried at 50 °C in a forced air oven. After 24 h, the temperature was raised to 180 °C and kept at that temperature for 90 min. The resulting corn-like silks were removed, allowed to cool, and washed in hot deionized water (60- 80 °C) until the liquid did not turn cloudy when mixed with 20 mL lead nitrate solution buffered to pH 4.8 in 0.03 M acetic acid and 0.07 M sodium acetate buffer. This washing step was aimed to remove free phosphate in the corn silk. The wet chitosan was dried at 50 °C for 24h, removed and stored for further examination.

Preparation of Nanochitosan

The reduction method used by Okafor *et al.* [24] was utilized to synthesize nanochitosan. Two grams of chitosan were dissolved in 50 mL of 1% acetic acid with constant stirring, and the pH of

the resulting solution was kept at 4 using 1M HCl. Additionally, 100 mg of sodium tripolyphosphate was dissolved in 100 mL of 1M NaOH, and the resulting solution was added to the mixture of acidified chitosan in drops with the help of a syringe until precipitates were fully formed. Using a homogenizer, the mixture was centrifuged at 1000 rpm for five minutes. A filter paper with a 0.2 µm pore size was used to filter the mixture. The nanochitosan was collected as the residue.

Characterization of Nanochitosan

Particle Size Analysis

The particle size distribution of the samples was measured by photon correlation spectroscopy (PCS) using a Malvern Zetasizer Nano ZS laser particle size analyzer following a protocol described by Akbari *et al.* [25] with modifications. The instrument was equipped with a He-Ne laser source wave length (wavelength = 633 nm) and at a scattering angle of 1730°. The dispersion concentration was around 0.1 g/L. The suspension was prepared by dispersing the powder in distilled water and treated for 60 mins in an ultrasonic bath to obtain a well-dispersed suspension.

Fourier Transform Infrared Analysis

Buck scientific M530 USA FTIR was used for the analysis. This instrument was equipped with a detector of deuterated triglycine sulphate and beam splitter of potassium bromide. The software of the Gram A1 was utilized to obtain the spectra and to manipulate them. Approximately 1.0 g of the sample was added to 0.5 mL of nujol, mixed properly and placed on a salt pellet. During measurement, FTIR spectra were obtained within the frequency range of 4,000 – 600 cm^{-1} and co-added at 32 scans and at 4 cm^{-1} resolutions. FTIR spectra were displayed as transmitter values.

Scanning Electron Microscopy (SEM) Analysis

The scanning electron microscopy (SEM) was performed to examine the physical structural changes of samples using SEM model (Phenom ProX, by phenomWorld Einhoven-the Netherlands). The sample was placed on double-sided adhesive which was on a sample stub, coated with a sputter coater by Quorum technologies model (Q150R) with a 5nm layer of gold. Thereafter, it was taken to the chamber of the SEM machine where it was viewed via NaVCaM for focusing and little adjustment. It was then transferred to the SEM mode, focused, and brightness and contrast were automatically adjusted; afterward, the morphologies of different magnifications were stored in a USB stick. After the morphology was acquired, its elemental composition was obtained via the software in the machine.

X-ray Diffraction (XRD) Analysis

The sample was prepared and compressed in the flat sample holder to create a flat, smooth surface that was later mounted on the sample stage in the XRD cabinet. The reflection-transmission spinner stage with theta-theta settings was employed to analyze the sample. With a two-theta step of 0.026261 at an average speed of 8.67 seconds per step, the two-theta starting position was 4° and ended at 75°. The tension was 45 VA, and the tube current was set at 40 mA. A Programmable divergent slit with a 5 mm width mask and Gonio Scan were used. The intensity of diffracted X-rays was continuously recorded as the sample and detector rotated through their respective angles. The results were commonly presented as peak positions at 2θ and X-ray counts (intensity).

Removal of PAHs contaminated surface water by batch adsorption method

0.2 g of each nanochitosan was weighed in two separate conical flasks. 40 mL of the contaminated water sample was measured and poured into each of the conical flask containing the modified chitosan particles. The orbital shaker was turned on and flasks contai**ni**ng the samples were placed on it to stand for 1hour at room temperature and the speed of 200 rpm. After 1hour, the samples were taken off from the shaker and filtered. The filtrates were taken for further analysis.

Extraction and analysis of PAHs in water samples

The method used by Okafor *et al.* [2] was adopted for the extraction and analysis of the water samples. All water samples were extracted without filtering to reflect exposure levels of PAHs in the water samples. A separating funnel was used for the extraction of PAHs from the water samples. The extraction of water samples and their spiked duplicates for PAHs followed a common procedure: 250 mL of separating funnel containing 100 mL of an equal mixture of chromatographic grade DCM/n-hexane. The samples were extracted for 2 hours under reflux. The crude extracts were concentrated to a volume of nearly 2 mL using a rotary vacuum

evaporator. The resulting concentrates were purified NY short-column silica gel chromatography using DCM as the eluting solvent. The eluates were further reduced to a final volume (2 mL) using nitrogen gas and reconstituted with 2 mL of chromatographic-grade isooctane. The purified extracts (in sealed vials) were kept in the fridge until conducting analysis by GC- FID.

The samples were analyzed with 7890A Agilent Gas chromatograph coupled with a HP5 column (30m x 0.32mm x 0.25um). 1 µL was injected into the GC for the determination of PAH under the following oven condition:

Initial Temp: 60'C, Held for 1min
Ramp rate 1: Increased to 210'C @ 12'C/min
Ramp rate 2: Increased to 320'C @ 8'C/min
(Final Temp.) Held 5mins
Total run time: 32.25mins
Detector Temp: 325'C

The concentration of analytes was determined by the peak area of samples against those of the standard with which the equipment was calibrated.

RESULTS AND DISCUSSION

Dynamic Light Scattering (DLS) Analysis

The Brownian motion of particles in a dispersion is used in DLS analysis to determine particle size. When a particle suspension is subjected to a monochromatic wave of light, the wavelength of the light changes after striking the particles, and a detector detects the signal.

Four samples were analyzed for particle sizes in order to compare the differences in the sizes of chitosan extracted from C*ambarus bartonii* (CbC), nanochitosan prepared from CbC (CbNC), low molecular weight artificial chitosan (ArC), and nanochitosan prepared from ArC (ArNC). Table 1 shows the results of the particle sizes of the four products.

The results indicated that there was actually a reduction in size from chitosan to nanochitosan in the extracts. Sample CbC was reduced from 66.55 nm to 55.78 nm (CbNC), while ArC (92.64 nm) was reduced to 68. 82 nm (ArNC). The reduction in the particle sizes of CbC and ArC shows an increase in the surface area of the nanochitosan particles (CbNC and ArNC). The results of DLS in the present work are in good agreement with the results reported by Yusefi *et al.* [26].

Table 1 Particle size of the extracts.

Extract	Particle size (nm)
CbC	66.55
CbNC	55.78
ArC	92.64
ArNC	68.82

Fourier Transform Infrared (FTIR)

FTIR provides information on the chemical structure of the carbon material. FTIR studies were conducted to reveal the probable chemicals contributing to the reduction of nanoparticles. Tables 2 and 3 illustrate the peak wavelengths and functional groups of CbNC and ArNC, respectively. The carbon matrix of organic substances like chitosan does not consist of carbon atoms alone, but is also formed by other hetero-atoms like hydrogen, oxygen, nitrogen, halogens, sulphur, phosphorus, etc. These hetero-atoms are bonded to the edges of the carbon layers which govern the surface chemistry of the adsorbent sample which are detected in both CbNC and ArNC, enabling them to act as an adsorbent. The peaks at 2646.4 cm^{-1}, 2325.9 cm^{-1} and 2284.9 cm^{-1} in ArNC indicate the presence of -O-H in phosphorus and oxyacids, and P-H in phosphines, respectively, showing the abundance of heteroatoms. ArNC containing more of these hetero-atoms bonded to their carbon layers as indicated in the FTIR spectra (Figs. 1 and 2) is expected to behave as a better adsorbent compared to CbNC. These results align favorably with those obtained by Divya *et al.* [27], Rubini *et al.* [28] and Alshehri *et al.* [29]. Moreover, the results obtained by Okafor and his coworkers [23, 24] were in agreement with the result of this study.

The bands at 2,922.2 cm^{-1} and 1405.2 cm^{-1} represent C–H and C–N groups, respectively, which clearly indicate the absorption spectrum of chitosan [30] and the band at 1025.0 cm^{-1}, stretches C–O–C groups [31]. Furthermore, other researchers have also reported FTIR spectrum for chitosan nanoparticles revealing some variations in the obtained data [32 – 36].

Scanning Electron Microscopy (SEM)

SEM analysis demonstrated that the nanochitosan particles had a long thin crystal structure on a non-smooth surface with interconnected granular microporosity (Figs. 1

Table 2: FTIR of CbNC

Wavenumber (cm^{-1})	Functional group/mode of vibration	Inference
3678.9	Strong, -OH stretch peak	-OH, in Alcohols and Phenols
3421.7		
3265.1		
2922.2	Medium-strong, $-CH_3$ and $-CH_2-$, CH atisym and sym stretching peak	CH in Aliphatic compounds
2117.1	Weak-medium, C≡C stretch peak	C≡C in alkynes
1759.3	Strong, C=O stretch peak	C=O in carbonyl compounds
1654.9		
1617.7	Strong, C=C stretch peak	C=C in vinyl ethers
1558.0	Medium, NH_2 deformation peak	NH_2 in primary alkyl amide
1405.2	Medium, C-N stretch peak	C-N in primary amides
1312.0	Medium-strong, CF_3 antysm stretch peak	$-CF_3$ attached to benzene ring
1203.9	Strong, C-O-C antysm stretch peak	C-O-C in vinyl ethers
1151.7	Strong, SO_2 sym stretch peak	SO_2NH_2 in sulfonamides
1025.0	Very strong, C=O stretch peak	$-CH_2$-OH in primary alcohols
954.2	Strong, CH out-of-plane deformation peak	$CH_2=CH_2$ in vinyl compounds
872.2	Very strong, CH_2 out-of-plane wag	$CH_2=CR_2$ in vinylidenes
685.8	Strong, CH out-of-plane deformation peak	$CH_2=CH_2$ in cis disbust alkenes

and 2). This was in accordance with the findings of Mohanasrinivasan *et al.* [37] that reported a non-homogenous and non-smooth surface structure of nanochitosan in their work. Interconnected granular microporosity was observed more in ArNC favoring its effectiveness as an adsorbent in comparison with CbNC. Chitosan with a long, thin crystal structure on a smooth surface was also reported [38].

X-ray Diffraction

X-ray diffraction is known to be a non-destructive technique that works effectively with materials that are wholly or partly crystalline. Figs. 3 and 4 illustrate that CbNC and ArNC have four and three distinct sharp characteristics diffraction peaks, respectively. The peaks at $2\theta = 8.20^{o}$, 32.08^{o}, 38.00^{o} and 45.76^{o} correspond to CbNC, while those at $2\theta = 20.21^{o}$, 31.63^{o} and 45.48^{o} are attributed to ArNC.

The sharper peaks provide evidence of a denser crystalline structure [29]. The characteristic peaks of chitosan are reported in the ranges of 2θ= 9.9 - 10.7 and 19.8 - 20.7 [39]. Furthermore, the crystalline nature of shrimp-derived chitosan nanoparticles was determined by the most intense

Table 3: FTIR of ArNC.

Wavenumber (cm^{-1})	Functional group/mode of vibration	Inference
3652.8	Strong, OH stretch peak	OH, in Alcohols and Phenols
3399.3	Medium-strong, NH stretch peak	NH_2 in aromatic amines, primary amines and amides
3287.5	Medium, OH stretch peak	OH in Oximes
3205.5	Strong, NH_2 sym stretch	NH_2 in primary amides
2922.2	Medium-strong, -CH_3 and –CH_2-, CH atisym and sym stretching peak	CH in Aliphatic compounds
2646.4	Medium, OH stretching peak	OH in Phosphorus Oxyacids
2467.5	Very broad, H-bonded OH stretch peak	OH in carboxylic acids
2374.3	Broad, NH stretching mode peak	NH_3^+ in amine hydrohalides
2325.9	Medium, P-H stretch sharp peak	PH in phosphines
2284.9		
2199.1	Weak-medium, C≡C stretch peak	C≡C in alkynes
2005.9	Substituted benzene ring	Several bands from overtone and combination bands
1982.9	Strong, C=C=C antysm stretch peak	C=C=C in allenes
1871.1	Very strong, C=O stretch peak	C=O in carbonyl compounds
1796.6		
1654.9	Very strong, C=O stretch peak	C=O in primary amides
1565.5	Strong, ring stretch peak	Pyridine derivatives
1379.1	Strong, CH_3 sym deformation peak	CH_3 in aliphatic compounds
1148.0	Strong, SO_2 sym stretch	SO_2NH_2 in sulfonamides
1021.3	Strong, C-O stretch peak	CH-O-H in cyclic alcohols
879.7	Very strong CH out-of-plane deformation	1,1,4-trisubst benzenes
842.4	Very strong CH out-of-plane deformation	1,3,5-trisubst benzenes

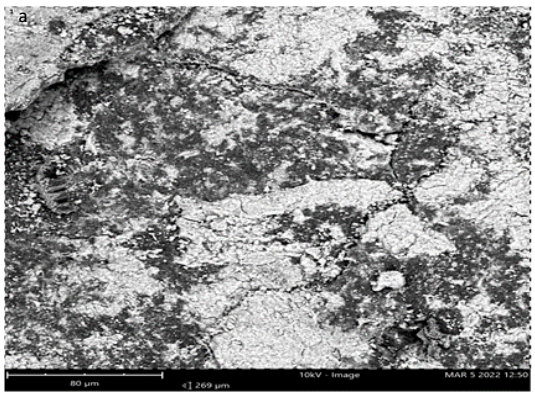

Fig. 1: SEM micrograph of CbNC

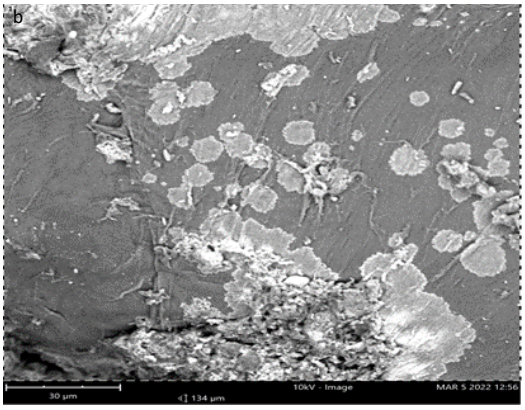

Fig. 2: SEM micrograph of ArNC

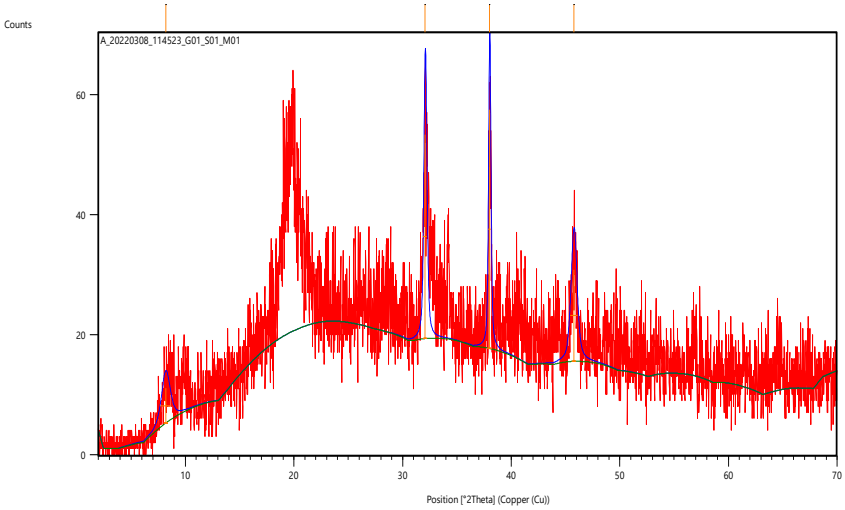

Fig. 3: Diffraction peak of nanochitosan from *C. bartonii*

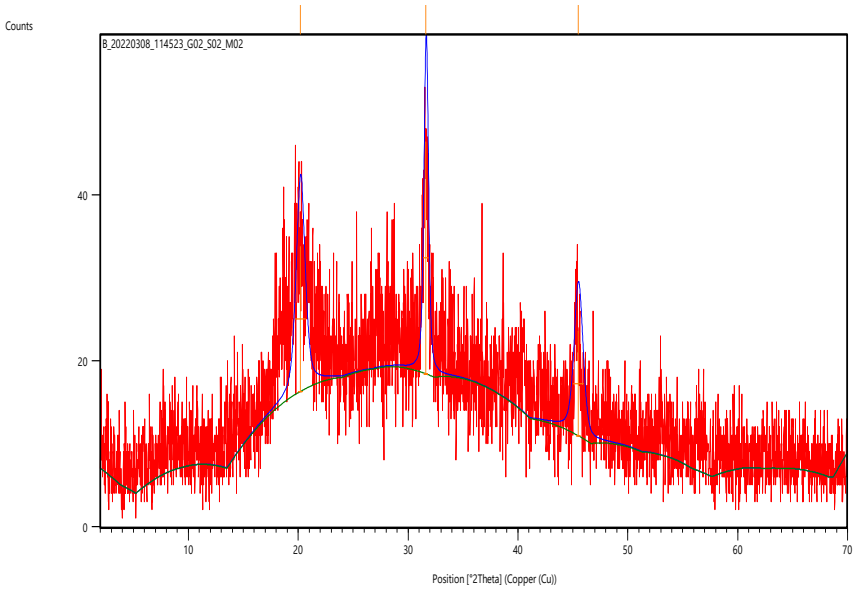

Fig. 4: Diffraction peak of nanochitosan from artificial chitosan

Table 4 PAHs values from the water samples.

PAHs	UWS (ng/µl)	WCbNC (ng/µl)	WArNC (ng/µl)
Naphthalene (Nap)	5.2968	ND	ND
Acenaphthene (Acy)	ND	ND	ND
Acenaphthylene (Ace)	ND	ND	ND
Fluorene (Flu)	ND	ND	ND
Phenanthrene (PA)	ND	ND	ND
Anthracene (Ant)	ND	ND	ND
Fluoranthene (Flt)	4.0358	ND	ND
Pyrene (Py)	ND	ND	ND
Benzo[a]anthracene (BaA)	4.0700	ND	ND
Chrysene (Cry)	82.4078	ND	ND
Benzo[k]fluoranthene (BkF)	5.2636	ND	ND
Benzo[b]fluoranthene (BbF)	21.1336	ND	ND
Benzo[a]pyrene (BaP)	3.4669	ND	ND
Dibenzo[a,h]anthracene (DBA)	23.5052	ND	ND
Indeno[1,2,3-cd] pyrene (IND)	ND	ND	ND
Benzo[ghi]perylene (BghiP)	11.8185	ND	ND
Σ PAHs	160.9882	-	-

ND: Not detected

diffraction peaks at values of 11.7 and 20.2° [40]. The difference in the number of diffraction peaks in the two nanochitosan particles indicates that ArNC has denser crystalline structure than CbNC. However, the XRD diffraction patterns obtained by Thamilarasan *et al.* [41] were located at 2θ = 12.67°, 19.04°, 23.27°, 26.37°, 34.83° and 39.24° which do not align with the findings presented by Zahedi *et al.* [40]. Nevertheless, these results favorably agree with the findings reported by Okafor *et al.* [24] who obtained similar results in which diffraction peaks were located between 2θ = 8.1° and 20.1 ° for chitosan particles and at 2θ =33.6°, 43.33° and 46.5° for Ag-nanoparticles.

PAHs analysis

Three water samples were analyzed for the 16 USEPA priority PAHs namely: untreated water sample (UWS) from Isiachala stream in Ifite Ogwari, South-East Nigeria, water sample from Isiachal stream treated with CbNC (WCbNC), and water sample from Isiachala treated with ArNC (WArNC).

The fingerprint (GC chromatogram) of UWS is represented in Fig. 5, while those of WCbNC and WArNC are illustrated in supplementary Figs. S1 and S2, respectively. It is evident from the fingerprints that 9 PAHs (∑PAHs = 160.9882 ng/ml) were contained in the untreated water sample (UWS) out of the 16 SEPA priority PAHs from Isiachala stream, while none of the PAHs was detected in WCbNC and WArNC as presented in Table 4.

Most of the published literature on the effects

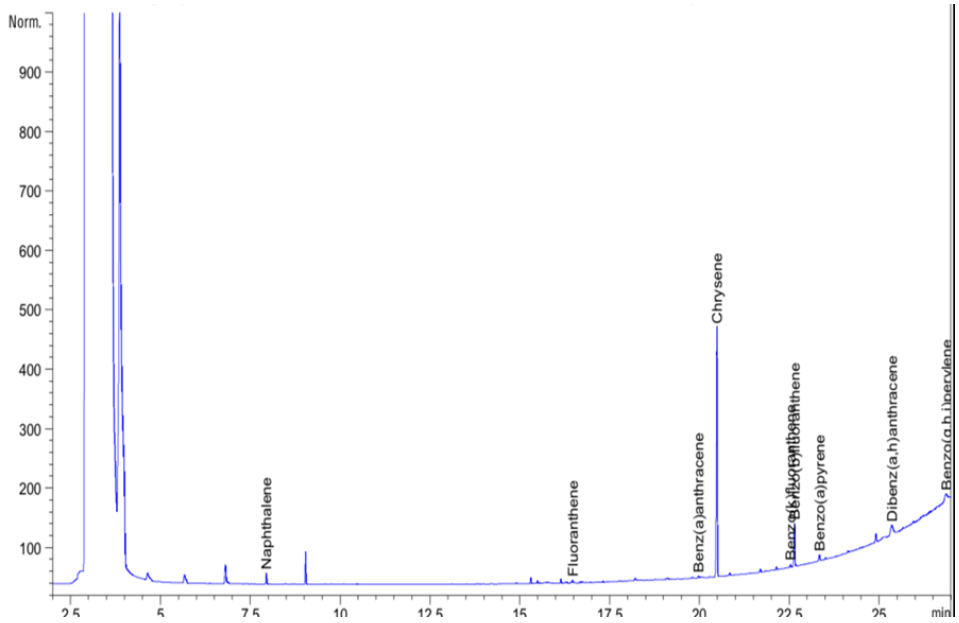

Fig. 5: Fingerprint of UWS.

of PAHs on human health has mainly focused on their potential to cause cancers of the skin, lung, breast, scrotum, bladder, and colon, etc. [42, 43]. According to Patel *et al.* [13], PAHs are byproducts of human activity such as forest fires, household and commercial heating appliances, companies and power plants that produce energy and volcanic activity. As a result, they have been detected in water, air, soil, and agricultural products [44]. PAHs in the environment are transferred to these substrates due to direct contact or as a result of precipitation [45].

If inhaled or ingested in high amounts, naphthalene can destroy red blood cells [46]. Flt has also been linked to liver and lung cancers [47], T cell apoptosis [48], a drop in white blood cell counts, and tubular casts in the kidneys [49]. Ugochukwu and Ochonogor reported benzo(a) anthracene's carcinogenic adverse health effects [50]. For the first time, Tao *et al.* [51] demonstrated that chrysene exposure damages the liver by activating the aryl hydrocarbon receptor, and that chrysene also protects against oxidative liver damage by activating the nuclear factor erythroid 2-related factor-mediated antioxidant defense mechanism. Benzo[k]fluoranthene (BkF) is known to accelerate the catabolism of 17 estradiol (E2) in human breast cancer cells, according to a study by Arcaro et al. [52]. Women who work in air-polluted BbF environments, such as petrochemical plants and busy roadways, are more likely to have irregular menstrual cycles, aberrant hormone levels, and a greater risk of infertility [53–55]. BbF exposure raises the likelihood of developing cancer [56], causes renal and lung illnesses, and exhibits high reproductive toxicity [57, 58]. Benzo[a]pyrene consumption at high levels during pregnancy has been linked to birth abnormalities and reduced body weight in mouse pups, according to Allamandola [14]. Although it has not been demonstrated that this impact occurs in humans, higher levels of PAH exposure during pregnancy are linked to undesirable birth outcomes, such as low birth weight, premature birth, and heart deformity [59].

High parental exposure is also associated with lower intelligent quotient at age three, increased behavior problems at age six and eight, and childhood asthma. Cord blood of exposed babies show DNA damage that has been linked to cancer [60]. Dibenzo[a,h]anthracene was reported as the most potent carcinogenic [61] as there were no oral or inhalation effects available to assess the carcinogenicity of benzo[ghi]perylene. The result reported for dermal came out negative [62, 63]. It was also reported that benzo[ghi]perylene

was administered alongside benzo[a]pyrene to a skin of a mice, and a skin tumor was observed compared to the tumor incidence in mice treated with benzo[a]pyrene alone. This indicates possible carcinogenicity present in benzo[ghi]perylene [64].

The study has demonstrated that nanochitosan particles obtained from *C. bartonii* could remove all the above PAHs, with the aforementioned health challenges in some rural communities in Nigeria that lack potable water.

Proposed mechanism of PAHs adsorption

The mechanism for PAHs adsorption onto artificial and natural nanochitosan could be proposed based on the functional groups as revealed by Infrared analysis. The protonated amino groups from chitosan (NH_3^+) and the π-electron-rich aromatic structures of the PAHs may interact cationically during the adsorption of PAHs on chitosan-nanoparticles. The adsorption of PAHs may also involve electrostatic interactions and hydrogen bonding due to the presence of amine and hydroxyl group on the adsorbents. The encouraging adsorption results of artificial and natural nanochitosan particles may be attributed to an intramolecular donor–acceptor interaction between the chitosan functional groups and PAHs [65,66].

CONCLUSIONS

The data concerning particle sizes reveal that nanochitosan particles from C*ambarus bartonii* waste and artificial chitosan have lesser sizes than the chitosan extracted from C*ambarus bartonii* waste and artificial chitosan, respectively. This means that modification was able to decrease the size of the nanochitosan particles. The FTIR analysis shows that carbon matrix of the nanochitosan particles consists of not only carbon atoms, but also other hetero-atoms like hydrogen, oxygen, nitrogen, halogens, sulphur, phosphorus, etc. confirmed by the observed FTIR peaks at 2646.4 cm^{-1}, 2325.9 cm^{-1}, 2284.9 cm^{-1} etc. Nanochitosan particle from artificial chitosan containing more of these hetero-atoms bonded to their carbon layers as indicated in the FTIR is expected to behave as a better adsorbent compared to the nanochitosan particle from C*ambarus bartonii*. The significant difference in the morphologies of the nanochitosan particles from C*ambarus bartonii* and artificial chitosan shows that the interconnected granular microporosity was observed more in the nanochitosan particle from artificial chitosan, favoring its effectiveness as an adsorbent in comparison with nanochitosan particle from C*ambarus bartonii* waste.

Nanochitosan particles from C*ambarus bartonii* waste and artificial chitosan have four and three distinct sharp characteristics diffraction peaks, respectively. The peaks at 2θ = 8.20°, 32.08°, 38.00° and 45.76° are related to nanochitosan particle from C*ambarus bartonii,* waste while those at 2θ = 20.21°, 31.63° and 45.48° correspond to nanochitosan particle from artificial chitosan. The difference in the intensities in the two products indicates that nanochitosan particle from artificial chitosan has denser crystalline structure than nanochitosan particle from C*ambarus bartonii* waste.

PAHs were present in the surface water sample collected from Isiachala stream in Ifite Ogwari community. This implies that the surface water is not suitable for drinking unless treated. The minimum and maximum concentrations of PAHs in the surface water from Ifite Ogwari were 3.4669 ng/ml (Benzo[a]pyrene) and 82.4078 ng/ml (Chrysene), respectively, and ∑PAHs = 160.9882 ng/ml. The water samples treated with both nanochitosan particles did not indicate the presence of any of the PAHs in them. This implies that the nanochitosan particle from C*ambarus bartonii* waste could treat PAHs contaminated surface water in the same manner as the artificial chitosan.

In order to reduce exposure to PAHs in the environment, regulatory agencies should regularly monitor and ensure proper water treatment since PAHs are teratogenic, carcinogenic, and mutagenic, and may induce lung, bladder as well as skin cancer. Again, further studies should be carried out on the possibility of using natural raw materials in the extraction of chitosan for use in the treatment of water resources in Nigeria's rural communities.

ACKNOWLEDGMENTS

The authors would like to thank Nnamdi Azikiwe University for supporting the work and the technical staff of Central Laboratory, Nigerian Institute for Oceanography and Marine Research, Victoria Island, Lagos for technical assistance.

CONFLICT OF INTEREST

The authors declare no conflicts of interest.

REFERENCES

1. Kumar A, Xagoraraki I. Pharmaceuticals, personal care products and endocrine-disrupting chemicals in U.S. surface and finished drinking waters: A proposed ranking system.

Science of The Total Environment. 2010;408(23):5972-89. https://doi.org/10.1016/j.scitotenv.2010.08.048
2. Okafor VN, Omokpariola DO, Igbokwe EC, Theodore CM, Chukwu NG. Determination and human health risk assessment of polycyclic aromatic hydrocarbons (PAHs) in surface and ground waters from Ifite Ogwari, Anambra State, Nigeria. International Journal of Environmental Analytical Chemistry.1-23. https://doi.org/10.1080/03067319.2022.2038587
3. Okafor VN, Omokpariola DO, Obumselu OF, Eze CG. Exposure risk to heavy metals through surface and groundwater used for drinking and household activities in Ifite Ogwari, Southeastern Nigeria. Applied Water Science. 2023;13(4):105. https://doi.org/10.1007/s13201-023-01908-3
4. Bando D, Ikwebe J, Jummai T, Sunday O, Odiba O, David EH, et al. Heavy metal and polyaromatic hydrocarbon depositions on local kitchen and roadside sun-dried agricultural products in Nigeria: A public health concern. International Journal of Advanced Biochemistry Research. 2022;3.
5. Sampaio GR, Guizellini GM, da Silva SA, de Almeida AP, Pinaffi-Langley ACC, Rogero MM, et al. Polycyclic Aromatic Hydrocarbons in Foods: Biological Effects, Legislation, Occurrence, Analytical Methods, and Strategies to Reduce Their Formation. International journal of molecular sciences. 2021;22(11). https://doi.org/10.3390/ijms22116010
6. Olutona GO, Arigbedede OE, Dawodu MO. Polycyclic Aromatic Hydrocarbons (PAHs) and Trace Metals in Some Brands of Sausage Roll in the Nigerian Markets. Iranian Journal of Chemistry and Chemical Engineering. 2022;41(2):464-81.
7. Okafor VN, Uche UB, Abailim RC. Levels of Polycyclic Aromatic Hydrocarbons (PAHs) in Beers: Consumption and Public Health Concerns. Chemical Science International Journal. 2020;29(1):47-59. https://doi.org/10.9734/CSJI/2020/v29i130157
8. Okafor VN, Umennadi PU, Odidika CC, Vinna DC. METALS AND POLYCYCLIC AROMATIC HYDROCARBONS (PAHs) IN BEER: A REVIEW. Journal of Chemical Society of Nigeria. 2021;46(4). https://doi.org/10.46602/jcsn.v46i4.646
9. Okafor VN, Omokpariola DO, Okabekwa CV, Umezinwa EC. Heavy Metals in Alcoholic Beverages Consumed in Awka, South-East Nigeria: Carcinogenic and Non-carcinogenic Health Risk Assessments. Chemistry Africa. 2022;5(6):2227-39. https://doi.org/10.1007/s42250-022-00477-3
10. Okafor VN, Omokpariola DO, Agu MO, Odidika CC, Okabekwa CV, Ogbuo LC, et al. Assessment of polycyclic aromatic hydrocarbons (PAHs) in alcoholic beverages consumed in Awka, Southeast Nigeria. Bulletin of the Chemical Society of Ethiopia. 2023;37(4):805-15. https://doi.org/10.4314/bcse.v37i4.1
11. Di Bella C, Traina A, Giosuè C, Carpintieri D, Lo Dico GM, Bellante A, et al. Heavy Metals and PAHs in Meat, Milk, and Seafood From Augusta Area (Southern Italy): Contamination Levels, Dietary Intake, and Human Exposure Assessment. 2020;8. https://doi.org/10.3389/fpubh.2020.00273
12. Onopiuk A, Kołodziejczak K, Szpicer A, Wojtasik-Kalinowska I, Wierzbicka A, Półtorak A. Analysis of factors that influence the PAH profile and amount in meat products subjected to thermal processing. Trends in Food Science & Technology. 2021;115:366-79. https://doi.org/10.1016/j.tifs.2021.06.043
13. Patel AB, Shaikh S, Jain KR, Desai C, Madamwar D. Polycyclic Aromatic Hydrocarbons: Sources, Toxicity, and Remediation Approaches. 2020;11. https://doi.org/10.3389/fmicb.2020.562813
14. Allamandola L. Cosmic distribution of chemical complexity. NASA. 2011;Archived from the original on 2014-02-27.
15. Abdel-Shafy HI, Mansour MSM. A review on polycyclic aromatic hydrocarbons: Source, environmental impact, effect on human health and remediation. Egyptian Journal of Petroleum. 2016;25(1):107-23. https://doi.org/10.1016/j.ejpe.2015.03.011
16. Elieh-Ali-Komi D, Hamblin MR. Chitin and Chitosan: Production and Application of Versatile Biomedical Nanomaterials. International journal of advanced research. 2016;4(3):411-27.
17. Jiménez-Gómez CP, Cecilia JA. Chitosan: A Natural Biopolymer with a Wide and Varied Range of Applications. Molecules [Internet]. 2020; 25(17). https://doi.org/10.3390/molecules25173981
18. Aspden TJ, Mason JDT, Jones NS, Lowe J, Skaugrud Ø, Illum L. Chitosan as a Nasal Delivery System: The Effect of Chitosan Solutions on in Vitro and in Vivo Mucociliary Transport Rates in Human Turbinates and Volunteers. Journal of Pharmaceutical Sciences. 1997;86(4):509-13. https://doi.org/10.1021/js960182o
19. Petronela N. Applications of Chitosan in Wastewater Treatment. In: Emad AS, editor. Biological Activities and Application of Marine Polysaccharides. Rijeka: IntechOpen; 2017. p. Ch. 10.
20. Poureini F, Nikzad M. Application of Chitosan for wastewater treatment2015.
21. Vakili M, Rafatullah M, Salamatinia B, Abdullah AZ, Ibrahim MH, Tan KB, et al. Application of chitosan and its derivatives as adsorbents for dye removal from water and wastewater: a review. Carbohydrate polymers. 2014;113:115-30. https://doi.org/10.1016/j.carbpol.2014.07.007
22. Okoya A, Akinyele A, Amuda O, Ofoezie E. Chitosan Grafted Modified Maize Cob for Removal of Lead And Chromium from Wastewater. Ethiopian Journal of Environmental Studies and Management. 2016;8:881. https://doi.org/10.4314/ejesm.v8i2.3S
23. Okafor V, Umenne C, Blessing T, Okonkwo C, Obiefuna J, Okafor U, et al. Potentiality of Diethylamine as Agent of Deproteination and Deacetylation in the Extraction of Chitosan from Scylla serrata Shell. Chemistry and Materials Research. 2020;Vol. 12:35-45.
24. Okafor VN, Akinyele Abimbola B, Daberechukwu Iwe A, Mbume OF. Comparative Studies of Chitosan-Silver Nanocomposites from Commercial and Biowaste Sources. Nanochemistry Research. 2023;8(1):78-86.
25. Akbari B, Tavandashti MP, Zandrahimi M. PARTICLE SIZE CHARACTERIZATION OF NANOPARTICLES - A PRACTICALAPPROACH. IUST. 2011;8(2):48-56.
26. Mostafa Y, Pooneh K, Siti Nur Amalina Mohamad S, Roshafima Rasit A, Kamyar S. Synthesis and Properties of Chitosan Nanoparticles CrossLinked with Tripolyphosphate. Journal of Research in Nanoscience and Nanotechnology. 2021;3(1):46-52. https://doi.org/10.37934/jrnn.3.1.4652

27. Divya K, Rebello S, JishaM. S, editors. A Simple and Effective Method for Extraction of High Purity Chitosan from Shrimp Shell Waste2014.
28. Rubini D, Farisa Banu S, Veda Hari BN, Ramya Devi D, Gowrishankar S, Karutha Pandian S, et al. Chitosan extracted from marine biowaste mitigates staphyloxanthin production and biofilms of Methicillin- resistant Staphylococcus aureus. Food and Chemical Toxicology. 2018;118:733-44. https://doi.org/10.1016/j.fct.2018.06.017
29. Alshehri MA, Aziz AT, Trivedi S, Panneerselvam C. Efficacy of chitosan silver nanoparticles from shrimp-shell wastes against major mosquito vectors of public health importance. 2020;9(1):675-84. https://doi.org/10.1515/gps-2020-0062
30. Govindan S, Nivethaa EAK, Saravanan R, Narayanan V, Stephen A. Synthesis and characterization of chitosan-silver nanocomposite. Applied Nanoscience. 2012;2(3):299-303. https://doi.org/10.1007/s13204-012-0109-5
31. Saraswathy G, Pal S, Rose C, Sastry TP. A novel bio-inorganic bone implant containing deglued bone, chitosan and gelatin. Bulletin of Materials Science. 2001;24(4):415-20. https://doi.org/10.1007/BF02708641
32. Murugan K, Anitha J, Dinesh D, Suresh U, Rajaganesh R, Chandramohan B, et al. Fabrication of nano-mosquitocides using chitosan from crab shells: Impact on non-target organisms in the aquatic environment. Ecotoxicology and Environmental Safety. 2016;132:318-28. https://doi.org/10.1016/j.ecoenv.2016.06.021
33. Murugan K, Anitha J, Suresh U, Rajaganesh R, Panneerselvam C, Aziz AT, et al. Chitosan-fabricated Ag nanoparticles and larvivorous fishes: a novel route to control the coastal malaria vector Anopheles sundaicus? Hydrobiologia. 2017;797(1):335-50. https://doi.org/10.1007/s10750-017-3196-1
34. Murugan K, Jaganathan A, Suresh U, Rajaganesh R, Jayasanthini S, Higuchi A, et al. Towards Bio-Encapsulation of Chitosan-Silver Nanocomplex? Impact on Malaria Mosquito Vectors, Human Breast Adenocarcinoma Cells (MCF-7) and Behavioral Traits of Non-target Fishes. Journal of Cluster Science. 2017;28(1):529-50. https://doi.org/10.1007/s10876-016-1129-1
35. Kannan RRR, Arumugam R, Ramya D, Manivannan K, Anantharaman P. Green synthesis of silver nanoparticles using marine macroalga Chaetomorpha linum. Applied Nanoscience. 2013;3(3):229-33. https://doi.org/10.1007/s13204-012-0125-5
36. Ramkumar VS, Pugazhendhi A, Gopalakrishnan K, Sivagurunathan P, Saratale GD, Dung TNB, et al. Biofabrication and characterization of silver nanoparticles using aqueous extract of seaweed Enteromorpha compressa and its biomedical properties. Biotechnology Reports. 2017;14:1-7. https://doi.org/10.1016/j.btre.2017.02.001
37. Mohanasrinivasan V, Mishra M, Paliwal JS, Singh SK, Selvarajan E, Suganthi V, et al. Studies on heavy metal removal efficiency and antibacterial activity of chitosan prepared from shrimp shell waste. 3 Biotech. 2014;4(2):167-75. https://doi.org/10.1007/s13205-013-0140-6
38. Hwang JWSL. Synthesis and characterisation of chitosan from shrimp shell: UTAR; 2013.
39. Al-Sherbini AA, Ghannam HEA, El-Ghanam GMA, El-Ella AA, Youssef AM. Utilization of chitosan/Ag bionanocomposites as eco-friendly photocatalytic reactor for Bactericidal effect and heavy metals removal. Heliyon. 2019;5(6):e01980. https://doi.org/10.1016/j.heliyon.2019.e01980
40. Zahedi S, Safaei Ghomi J, Shahbazi-Alavi H. Preparation of chitosan nanoparticles from shrimp shells and investigation of its catalytic effect in diastereoselective synthesis of dihydropyrroles. Ultrasonics Sonochemistry. 2018;40:260-4. https://doi.org/10.1016/j.ultsonch.2017.07.023
41. Thamilarasan V, Sethuraman V, Gopinath K, Balalakshmi C, Govindarajan M, Mothana RA, et al. Single Step Fabrication of Chitosan Nanocrystals Using Penaeus semisulcatus: Potential as New Insecticides, Antimicrobials and Plant Growth Promoters. Journal of Cluster Science. 2018;29(2):375-84. https://doi.org/10.1007/s10876-018-1342-1
42. Menzie CA, Potocki BB, Santodonato J. Exposure to carcinogenic PAHs in the environment. Environmental Science & Technology. 1992;26(7):1278-84. https://doi.org/10.1021/es00031a002
43. Mastrangelo G, Fadda E, Marzia V. Polycyclic aromatic hydrocarbons and cancer in man. Environmental Health Perspectives. 1996;104(11):1166-70. https://doi.org/10.1289/ehp.961041166
44. Zhang Y, Zhang L, Huang Z, Li Y, Li J, Wu N, et al. Pollution of polycyclic aromatic hydrocarbons (PAHs) in drinking water of China: Composition, distribution and influencing factors. Ecotoxicology and Environmental Safety. 2019;177:108-16. https://doi.org/10.1016/j.ecoenv.2019.03.119
45. Organization WH. Guidelines for drinking-water quality: incorporating the first and second addenda: World Health Organization; 2022.
46. Diggs DL, Huderson AC, Harris KL, Myers JN, Banks LD, Rekhadevi PV, et al. Polycyclic Aromatic Hydrocarbons and Digestive Tract Cancers: A Perspective. Journal of Environmental Science and Health, Part C. 2011;29(4):324-57. https://doi.org/10.1080/10590501.2011.629974
47. Yamaguchi K, Near R, Shneider A, Cui H, Ju S-T, Sherr DH. Fluoranthene-Induced Apoptosis in Murine T Cell Hybridomas Is Independent of the Aromatic Hydrocarbon Receptor. Toxicology and Applied Pharmacology. 1996;139(1):144-52. https://doi.org/10.1006/taap.1996.0153
48. Wang J-S, Busby WF, Jr. Induction of lung and liver tumors by flouranthene in a preweanling CD-1 mouse bioassay. Carcinogenesis. 1993;14(9):1871-4. https://doi.org/10.1093/carcin/14.9.1871
49. Knuckles ME, Inyang F, Ramesh A. Acute and subchronic oral toxicity of fluoranthene in F-344 rats. Ecotoxicology and Environmental Safety. 2004;59(1):102-8. https://doi.org/10.1016/S0147-6513(03)00110-6
50. Ugochukwu UC, Ochonogor A. Groundwater contamination by polycyclic aromatic hydrocarbon due to diesel spill from a telecom base station in a Nigerian City: assessment of human health risk exposure. Environmental Monitoring and Assessment. 2018;190(4):249. https://doi.org/10.1007/s10661-018-6626-2
51. Tao L-P, Li X, Zhao M-Z, Shi J-R, Ji S-Q, Jiang W-Y, et al. Chrysene, a four-ring polycyclic aromatic hydrocarbon, induces hepatotoxicity in mice by activation of the aryl hydrocarbon receptor (AhR). Chemosphere. 2021;276:130108. https://doi.org/10.1016/j.chemosphere.2021.130108
52. Kathleen F. Arcaro YYJFGn. BENZO [k]FLUORANTHENE ENHANCEMENT AND SUPPRESSION OF 17BETA-ESTRADIOL CATABOLISM IN MCF-7

BREAST CANCER CELLS. Journal of Toxicology and Environmental Health, Part A. 1999;58(7):413-26. https://doi.org/10.1080/009841099157142
53. Thurston SW, Ryan L, Christiani DC, Snow R, Carlson J, You L, et al. Petrochemical exposure and menstrual disturbances. American Journal of Industrial Medicine. 2000;38(5):555-64. https://doi.org/10.1002/1097-0274(200011)38:5<555::AID-AJIM8>3.0.CO;2-E
54. Tomei G, Ciarrocca M, Fortunato BR, Capozzella A, Rosati MV, Cerratti D, et al. Exposure to traffic pollutants and effects on 17-β-estradiol (E2) in female workers. International Archives of Occupational and Environmental Health. 2006;80(1):70-7. https://doi.org/10.1007/s00420-006-0105-8
55. Mahalingaiah S, Hart JE, Laden F, Farland LV, Hewlett MM, Chavarro J, et al. Adult air pollution exposure and risk of infertility in the Nurses' Health Study II. Human Reproduction. 2016;31(3):638-47. https://doi.org/10.1093/humrep/dev330
56. Soltani N, Keshavarzi B, Moore F, Tavakol T, Lahijanzadeh AR, Jaafarzadeh N, et al. Ecological and human health hazards of heavy metals and polycyclic aromatic hydrocarbons (PAHs) in road dust of Isfahan metropolis, Iran. Science of The Total Environment. 2015;505:712-23. https://doi.org/10.1016/j.scitotenv.2014.09.097
57. Mass MJ, Abu-Shakra A, Roop BC, Nelson G, Galati AJ, Stoner GD, et al. Benzo[b]fluoranthene: tumorigenicity in strain A/J mouse lungs, DNA adducts and mutations in the Ki- ras oncogene. Carcinogenesis. 1996;17(8):1701-4. https://doi.org/10.1093/carcin/17.8.1701
58. Zhang Y, Liu D, Liu Z. The benzo[b]fluoranthene in the atmospheric fine particulate matter induces mouse glomerular podocytes injury via inhibition of autophagy. Ecotoxicology and Environmental Safety. 2020;195:110403. https://doi.org/10.1016/j.ecoenv.2020.110403
59. Lamichhane DK, Leem J-H, Kim H-C, Lee J-Y, Park M-S, Jung D-Y, et al. Impact of prenatal exposure to polycyclic aromatic hydrocarbons from maternal diet on birth outcomes: a birth cohort study in Korea. Public Health Nutrition. 2016;19(14):2562-71. https://doi.org/10.1017/S1368980016000550
60. Edwards Susan C, Jedrychowski W, Butscher M, Camann D, Kieltyka A, Mroz E, et al. Prenatal Exposure to Airborne Polycyclic Aromatic Hydrocarbons and Children's Intelligence at 5 Years of Age in a Prospective Cohort Study in Poland. Environmental Health Perspectives. 2010;118(9):1326-31. https://doi.org/10.1289/ehp.0901070
61. Igbiri S, Udowelle NA, Ekhator OC, Asomugha RN, Igweze ZN, Orisakwe OE. Polycyclic Aromatic Hydrocarbons In Edible Mushrooms from Niger Delta, Nigeria: Carcinogenic and Non-Carcinogenic Health Risk Assessment. Asian Pacific journal of cancer prevention : APJCP. 2017;18(2):437-47.
62. Hoffmann D, Wynder EL. Selective Reduction of Tumor-igenicity of Tobacco Smoke. II. Experimental Approaches12. JNCI: Journal of the National Cancer Institute. 1972;48(6):1855-68.
63. Van Duuren BL, Goldschmidt BM. Cocarcinogenic and Tumor-Promoting Agents in Tobacco Carcinogenesis2. JNCI: Journal of the National Cancer Institute. 1976;56(6):1237-42. https://doi.org/10.1093/jnci/56.6.1237
64. Van Duuren B, Katz C, Goldschmidt BJJNCI. Cocarcinogenic agents in tobacco carcinogenesis. 1973;51:703-5.
65. Solano RA, De León LD, De Ávila G, Herrera AP. Polycyclic aromatic hydrocarbons (PAHs) adsorption from aqueous solution using chitosan beads modified with thiourea, TiO2 and Fe3O4 nanoparticles. Environmental Technology & Innovation. 2021;21:101378. https://doi.org/10.1016/j.eti.2021.101378
66. Patiño-Ruiz DA, De Ávila G, Alarcón-Suesca C, González-Delgado ÁD, Herrera A. Ionic Cross-Linking Fabrication of Chitosan-Based Beads Modified with FeO and TiO2 Nanoparticles: Adsorption Mechanism toward Naphthalene Removal in Seawater from Cartagena Bay Area. ACS Omega. 2020;5(41):26463-75. https://doi.org/10.1021/acsomega.0c02984